STEM CELLS TRANSLATIONAL MEDICINE®

HUMAN CLINICAL ARTICLE

Stable Intracerebral Transplantation of Neural Stem Cells for the Treatment of Paralysis Due to Ischemic Stroke

GUANGZHU ZHANG,[a] YING LI,[b] JAMES L. REUSS,[c] NAN LIU,[b] CUIYING WU,[a] JINGPO LI,[e] SHUANGSHUANG XU,[e] FENG WANG,[e] THOMAS G. HAZEL,[f] MILES CUNNINGHAM,[g] HONGTIAN ZHANG,[a] YIWU DAI,[a] PENG HONG,[a] PING ZHANG,[a] JIANGHONG HE,[a] HUIRU FENG,[h] XIANGDONG LU,[h] JOHN L. ULMER,[d] KARL K. JOHE,[f] RUXIANG XU[a]

[a]Affiliated BaYi Brain Hospital, Army General Hospital of PLA, Beijing, People's Republic of China; [b]Neurology Department, Army General Hospital of PLA, Beijing, People's Republic of China; [c]Prism Clinical Imaging, Inc., Milwaukee, Wisconsin, USA; [d]Department of Neuroradiology, Medical College of Wisconsin, Milwaukee, Wisconsin, USA; [e]Suzhou Neuralstem Biopharmaceutical Co., Ltd., Suzhou, People's Republic of China; [f]Neuralstem, Inc., Germantown, Maryland, USA; [g]Laboratory for Neural Reconstruction, McLean Hospital, Harvard Medical School, Belmont, Massachusetts, USA; [h]Department of Nuclear Medicine, Army General Hospital of PLA, Beijing, People's Republic of China

Correspondence: Karl K. Johe, Ph.D., Neuralstem, Inc., 20271 Goldenrod Lane, Germantown, Maryland 20876, USA. Telephone: +13013664850; e-mail: kjohe@neuralstem.com; or Xu Ruxiang, M.D., Affiliated BaYi Brain Hospital, Army General Hospital of PLA, Nan Men Cang No. 5, Dong Cheng District, Beijing, People's Republic of China. Telephone: (8610) 13810000416; e-mail: xuruxiang1123@163.com

Received October 9, 2018; accepted for publication May 10, 2019.

http://dx.doi.org/10.1002/sctm.18-0220

ABSTRACT

NSI-566 is a stable, primary adherent neural stem cell line derived from a single human fetal spinal cord and expanded epigenetically with no genetic modification. This cell line is being tested in clinical trials in the U.S. for treatment of amyotrophic lateral sclerosis and spinal cord injury. In a single-site, phase I study, we evaluated the feasibility and safety of NSI-566 transplantation for the treatment of hemiparesis due to chronic motor stroke and determined the maximum tolerated dose for future trials. Three cohorts (n = 3 per cohort) were transplanted with one-time intracerebral injections of 1.2×10^7, 2.4×10^7, or 7.2×10^7 cells. Immunosuppression therapy with tacrolimus was maintained for 28 days. All subjects had sustained chronic motor strokes, verified by magnetic resonance imaging (MRI), initiated between 5 and 24 months prior to surgery with Modified Rankin Scores [MRSs] of 2, 3, or 4 and Fugl-Meyer Motor Scores of 55 or less. At the 12-month visit, the mean Fugl-Meyer Motor Score (FMMS, total score of 100) for the nine participants showed 16 points of improvement (p = .0078), the mean MRS showed 0.8 points of improvement (p = .031), and the mean National Institutes of Health Stroke Scale showed 3.1 points of improvement (p = .020). For six participants who were followed up for 24 months, these mean changes remained stable. The treatment was well tolerated at all doses. Longitudinal MRI studies showed evidence indicating cavity-filling by new neural tissue formation in all nine patients. Although this was a small, one-arm study of feasibility, the results are encouraging to warrant further studies. STEM CELLS TRANSLATIONAL MEDICINE *2019;00:1–9*

SIGNIFICANCE STATEMENT

Several different cell types have been proposed and tested in preclinical models and clinical trials to treat neurological conditions. However, few have shown significant properties to differentiate into genuine neuronal phenotypes or capability to integrate into the central nervous system (CNS) tissue, which are expected to be prerequisite properties for long-lasting benefits. NSI-566 is an adherent neural stem cell line that differentiates, matures, and integrates into the CNS tissue. This study presents evidence supporting stable allogeneic neural tissue formation by the stem cells in the brains of chronic stroke patients, suggesting statistically significant clinical benefits from baseline as measured by three different validated stroke scales.

INTRODUCTION

Neural stem cells are the precursor cells present in the neuroepithelium along the neuraxis during mammalian fetal development [1]. Neuralstem, Inc. (NSI)-566, the investigational product used in this study, is a stable, primary cell line consisting of neural stem cells derived from a single human fetal spinal cord tissue and expanded only by epigenetic means with no genetic modification [2]. This cell line is being tested in clinical trials in the U.S. for treatment of amyotrophic lateral sclerosis (ALS; NCT01348451, NCT01730716) and spinal cord injury (SCI; NCT01772810; ClinicalTrials.gov identifier: NCT03296618). A variety of preclinical and clinical studies have demonstrated the therapeutic potential of NSI-566 for reversing paralysis due to various neurological etiologies.

Studies in ALS rodent models have shown that NSI-566 effectively engrafts in lesioned tissue, survives for many months, integrates into the host motor neuron circuitry, forms contacts on host motor neurons, and expresses multiple growth factors, resulting in decreased loss of α-motor neurons and increased lifespan [3–7]. In studies with rat contusion model of SCI, grafted NSI-566 survived in the necrotic tissue, proliferated to fill in the lesion cavity, and then

differentiated en masse into neurons, which were seen to project into the host tissue while the host neuronal fibers traversed across the human graft. Markers of mature human neurons, neurites, and synapses were colocalized with the host descending motor tracts [8, 9]. In another rat model of permanent paraplegia where the spinal cord was surgically transected at segment T3, intraspinal grafting of NSI-566 into the gap produced by the transection resulted in partial motor recovery. Histology showed NSI-566-derived neurons extending axons over 17 spinal segments. Formation of new relay circuits by the transplanted cells was thought to result in the improved function [10]. In a recent study of monkeys with hemitransection induced SCI, NSI-566 grafted into the lesion site demonstrated robust neuronal differentiation and long-distance axonal projections below the level of injury, which were shown to synapse with the monkey motor neurons in the segments caudal to the injury. The monkeys showed significant motor improvement, including hand manipulation [11].

Finally, two additional studies support a therapeutic role for NSI-566 in rodent models of ischemic injury. In a rat model of ischemic SCI in which ischemia-induced spasticity and rigidity accompanies permanent incomplete paraplegia, intraspinal grafting of NSI-566 into the lumbar gray matter resulted in progressive recovery of motor function and correlative improvement in motor evoked potentials over 2–3 months after grafting [12]. In rats with ischemic stroke induced by transient occlusion of the middle cerebral artery, NSI-566 transplantation into subcortical regions 7 days poststroke resulted in motor improvement in a dose-dependent manner [13]. Thus, NSI-566 has consistently demonstrated robust neuronal differentiation, maturation, integration, and survival for many months even in xenotransplantation when sufficient immunosuppression tolerated xenograft survival.

Three clinical studies have been conducted with NSI-566 allotransplantation: two ALS studies (n = 30) and one chronic SCI study (n = 4), amounting to a total of 34 participants, and 2–6 years of human safety/efficacy monitoring so far. These studies' results provide evidence that NSI-566 can survive in the host parenchyma for at least 2.5 years, even with transient immunosuppression, is safe, and can provide clinical benefits in patients with neurological damage [14–19]. Phases I and II ALS subjects who received NSI-566 showed significant functional stabilization as well as significantly better composite functional/survival score at 24 months compared with historical controls [18]. Furthermore, in a phase I study, three out of four complete paraplegic SCI patients with thoracic cord injuries who received NSI-566 transplantation exhibited new acquisition of voluntary muscle units and two of them showed neurological improvement below the level of injury [19].

Paralysis due to ischemic stroke is a major cause of prolonged neurological disability worldwide, particularly in China and other Asian countries [20]. There are currently no effective therapies to reverse stroke-associated paralysis. We have investigated the feasibility and safety of transplanting NSI-566 to reverse the paralysis in nine stably hemiparetic stroke patients.

Materials and Methods

Preparation of the Stem Cells

Details of NSI-566 derivation and manufacture have been previously described [16]. Briefly, NSI-566 is a stable line of expanded human neural stem cells derived from a single human fetal spinal cord tissue of approximately eight gestational weeks. No genetic modification was introduced to the cells. Concentrated, ready-to-inject cell doses from a clinical lot of passage 12 cells were prepared as live cell suspensions the day before surgery and couriered at 2°C–8°C to the transplantation surgery site in the morning of surgery. In this formulation, the product is usable for 48 hours from the time of preparation. The cell suspension was tested for acceptable cell viability (≥70%) by trypan blue exclusion method and administered into patients without further manipulation.

Participants

Between 2013 and 2016, potentially eligible subjects were selected from the hospital database, prescreened by telephone interview, underwent review of their medical and MRI records, and then received onsite screening. All nine subjects who met the initial screen eligibility received the stem cells treatment ("intent-to-treat" population). The participants were men and women 30–65 years old with hemiparesis from ischemic stroke and who remained stable based on National Institutes of Health Stroke Scale (NIHSS) assessments for at least 3 weeks prior to the surgery. All subjects had to have chronic motor deficit for at least 3 months but not more than 24 months from the time of stroke, with Modified Rankin Scores (MRSs) of 2, 3, or 4 and Fugl-Meyer Motor Scores of 55 or less, at the initial screening. All study participants were Chinese and signed informed consent form. As this was a feasibility study, no attempt was made to balance the gender. All transplantation surgeries and follow-up assessments were performed at BaYi Brain Hospital, Beijing, China, with approval by the hospital ethics committee.

Study Design

Three doses were tested: a total 1.2×10^7 cells (cohort A) distributed via 15 cell deposits, each consisting of 20 μl of 40,000 cells per microliter in three cannula tracks; a total 2.4×10^7 cells (cohort B) distributed via 15 cell deposits, each consisting of 20 μl of 80,000 cells per microliter in three cannula tracks; and a total 7.2×10^7 cells (cohort C) distributed via 45 cell deposits, each consisting of 20 μl of 80,000 cells per microliter in three cannula tracks. A straight cannula of Pittsburgh Design [21] was used for cohorts A and B (FHC, New Hampshire). A novel cannula design, intracerebral microinjection instrument with a side exit port was used for cohort C [22, 23] (FHC). Each successive dose had to be tolerated by all three patients before advancing to the next dose cohort. A safety monitoring board reviewed the safety of all patients prior to approving the next dose cohort. Follow-ups for the participants were planned for a period of 24 months post-transplantation and are reported here. Additional details of the methods used are provided in Supporting Information.

Results

Treatment Assignment

Nine participants in total were planned and enrolled successively in order of three dose cohorts of 12, 24, and 72 million cells (n = 3 per cohort, Table 1). All participants have completed 12–24 months of scheduled follow-up visits.

Demographics and Safety

The functional impairment for eight of nine subjects enrolled was of moderate disability, requiring some help but with the

Table 1. Treatment assignment

Cohort ID	Treatment	Cell number/deposit	No. of deposits/cannula track	No. of cannula tracks
A (n = 3)	12 million cells	40,000 cells per microliter × 20 μl	5	3
B (n = 3)	24 million cells	80,000 cells per microliter × 20 μl	5	3
C (n = 3)	72 million cells	80,000 cells per microliter × 20 μl	15	3

Table 2. Participant characteristics at baseline

Subject no.	Gender (F/M)	Age	Weight (kg)	Stroke location, volume (ml)[a]	Days poststroke[b]	NIHSS[c]	MRS[d]	FMMS[c]	Treatment cohort
101	M	50	78	Infarct, L, SC, 10.29	607	9	3	32	A
102	M	47	75	Infarct, R, SC, 6.44	424	2	3	29	A
103[e]	M	30	90	Infarct, R, SC, 4.17	150	5	3	39	A
104[e]	M	44	70	Infarct, R, SC, 7.01	519	10	3	19	B
105[e]	M	41	75	Infarct, R, SC, 71.15	357	7	3	41	B
106	M	45	75	Infarct, L, SC, 4.09	743	6	3	41	B
107	M	56	59	Infarct, L, SC, 13.31	417	7	4	27	C
108	M	38	71	Infarct, R, SC, 0.86	719	5	3	17	C
109	F	54	52	Infarct, R, SC, 0.81	517	6	3	48	C

[a]Volume was calculated in cubic centimeters from baseline T1 voxel counts in the lesion.
[b]At the time of stem cell administration.
[c]Determined at screen 2.
[d]Determined at screen 1 (not performed at screen 2).
[e]Withdrew consent after month 12 visit.
Abbreviations: F, female; FMMS, Fugl-Meyer Motor Score; L, left; M, male; MRS, Modified Rankin Scale; NIHSS, National Institutes of Health Stroke Scale; R, right; SC, subcortical.

ability to walk without assistance (Modified Rankin Scale [MRS] grade 3). The remaining subject (#107) was of moderately severe disability, unable to walk and unable to self-care without assistance (MRS grade 4). Motor deficit as determined by Fugl-Meyer Motor Score (FMMS, total score of 100), which had to be 55 or less for inclusion in the study, ranged from 19 to 48 among subjects. Three cases were of stroke in the left hemisphere and six cases were in the right hemisphere. The longest infarct dimension ranged from 17.2 to 86.6 mm. Subjects received the stem cell treatment 150–743 days poststroke event (Table 2).

The mean age of participants was 44 (minimum 30, maximum 54) with the mean NIHSS score of 6.3, mean FMMS (total 100) of 32.6, and mean MRS of 3.1. The baseline stroke characteristics were similar across the dose cohorts (Table 3).

Safety Assessments

Follow-up visits for safety and exploratory outcomes were scheduled at 1, 3, 6, 9, 12, and 24 months postoperative day of stem cell treatment. Safety assessments included computed tomography (CT) scan on the day of surgery or the following day to monitor potential hemorrhage, and at scheduled visits for physical exam, laboratory monitoring, and clinical stroke evaluations as well as periodic imaging studies by MRI.

There were 35 reported adverse events (AEs) during the study (Table 3). The injection times for 15 versus 45 cell deposits averaged 1:42 versus 4:32 (hour:minute). However, no increased AEs were apparent among the dose groups (18, 2, 15 for groups A, B, and C, respectively). Two subjects experienced serious AEs. One subject reported cholecystitis twice (shown in Supporting Information, Table S3). Related to CNS, there was one case of microcerebral hemorrhage (#102) detected by prescheduled CT scan, which required no intervention and resolved without sequelae. Two incidences of mild seizures (#101 and #102) were reported, which were treated with anti-seizure medications and resolved without sequelae.

All participants received 28 days of oral tacrolimus to maintain 4–8 ng/ml trough blood level for immunosuppression, as well as 14 days of prednisone postsurgery as an anti-inflammatory measure. Both drugs were well tolerated by all participants. All patients were discharged from the hospital after 14 days, as scheduled. Subsequent monitoring for appearance of antibodies against human leukocyte antigen (HLA) class I and II antigens was negative for all nine subjects.

Clinical Outcome

Twelve-month (n = 9) or 24-month (n = 6) follow-up data of the combined participants across the three dose groups were analyzed for clinical changes. Wilcoxon signed rank test was used. At the 12th month visit, the mean FMMS (total score of 100) showed 16.0 points of improvement from baseline (p = .0078, Fig. 1B). FMMS improvement was statistically significant at months 1, 3, 6, and 9 as well. The mean MRS at 12-month visit showed 0.8 points of improvement from baseline (p = .031, Fig. 1C). The MRS improvement was also statistically significant at months 3 and 9 as well. The mean NIHSS at 12-month visit showed a statistically significant improvement of 3.1 points from baseline (p = .020, Fig. 1D). The improvements were maintained at 24-month visit. The stem cell treatment was well tolerated at all doses. There was no occurrence of neurological worsening or treatment-related complications. The maximum tested dose of 7.2×10^7 cells was well tolerated with no more safety issues than the two lower cell doses.

Table 3. Mean demographics and safety results

	Cohort A (*n* = 3)	Cohort B (*n* = 3)	Cohort C (*n* = 3)	Pooled cohort (*n* = 9)
Age: mean (range)	42 (30–49)	43 (41–45)	48 (37–54)	44 (30–54)
Sex: male/female	3/0	3/0	2/1	8/1
NIHSS mean (SEM)	5.3 (2.0)	7.7 (1.2)	6.0 (0.6)	6.3 (0.8)
MRS mean (SEM)	3.0 (0.0)	3.0 (0.0)	3.3 (0.3)	3.1 (0.1)
FMMS mean (SEM)	33.3 (3.0)	33.7 (7.3)	30.7 (9.1)	32.6 (3.5)
AE/SAE/death reported	18/2[a]/0	2/0/0	15/0/0	35[b]/2/0

[a]Cholecystitis (grade 3), unrelated to surgery.
[b]Thirty-five total AEs involved seven subjects, of which 30 were resolved without sequelae, two incidences from cholecystitis were reported as having changed in status, and three continuing (#107 constipation; #108 pruritus and weight gain).
Abbreviations: AE, adverse event; FMMS, Fugl-Meyer Motor Score; MRS, Modified Rankin Scale; NIHSS, National Institutes of Health Stroke Scale; SAE, serious adverse event.

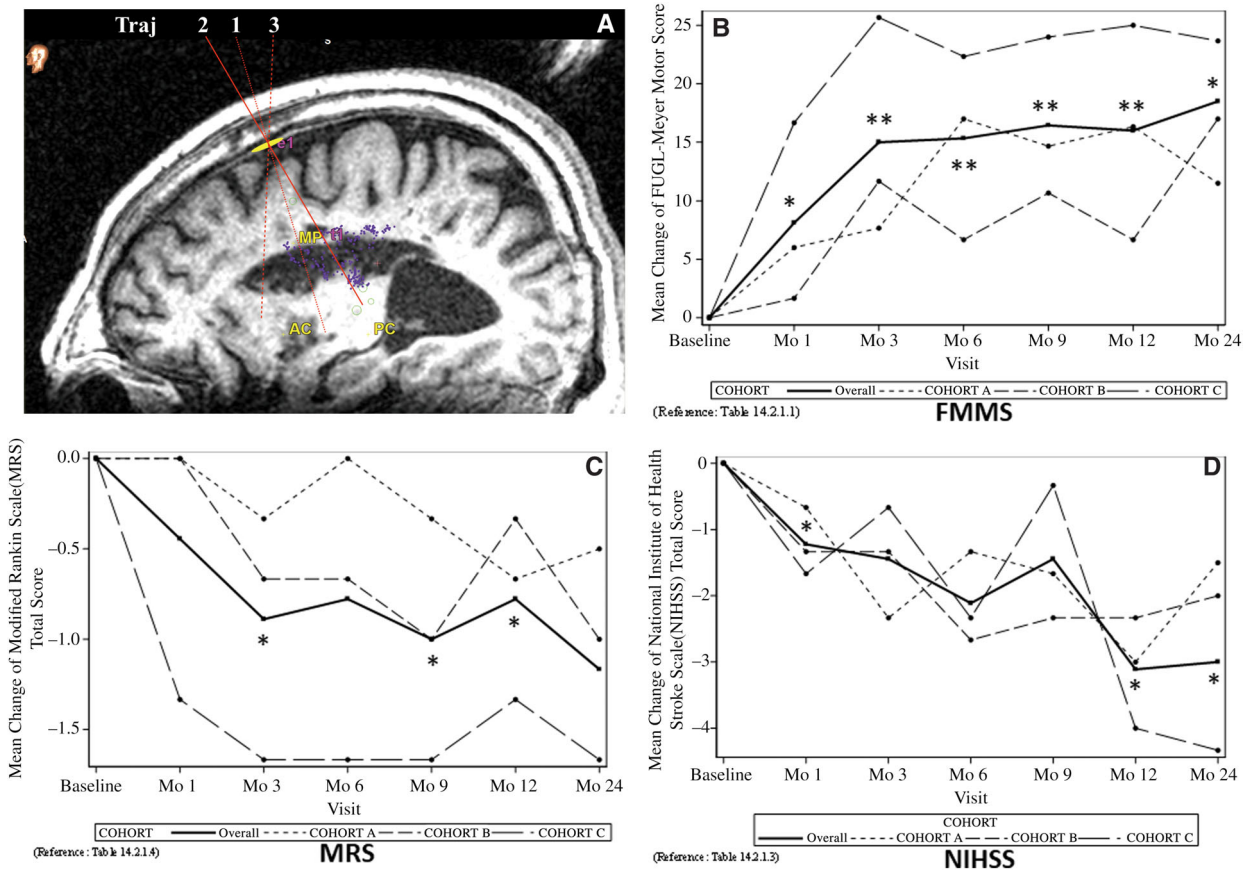

Figure 1. Clinical outcomes through 24-month visit. Score changes from the baseline are shown. **(A):** An illustration of the three cannula trajectories used for cell administration. **(B):** Fugl-Meyer Motor Score (mean ± SE). The functional motor score (total 100) at indicated visits postsurgery was subtracted from the baseline score obtained just prior to the stem cell treatment. *, $p < .05$; **, $p < .01$. **(C):** Modified Rankin Scale total score (mean ± SE). The score at indicated visits postsurgery was subtracted from the baseline score obtained just prior to the stem cell treatment. *, $p < .05$. **(D):** National Institutes of Health Stroke Scale (mean ± SE). The score at indicated visits postsurgery was subtracted from the baseline score obtained just prior to the stem cell treatment. *, $p < .05$. In (B)–(D), mean scores for cohorts (A–C) are also shown as indicated by the legend.

Imaging Studies

The imaging studies of nine subjects used in this study corroborate the clinical outcomes observed. Evidence of mature hemorrhage and encephalomalacia with formation of cerebrospinal fluid-filled cavity along the presumed implantation needle tract, but separate from the infarct cavity, was observed on postprocedural MRI in one subject. Otherwise, there were no sequelae of acute postprocedural complications observed.

New tissue was observed in all nine subjects by the 6-month follow-up, emanating from encephalomalacia infarct cavities. This intracavitary tissue appearance was characterized by the following criteria: short-term viability (tissue appearance at first postprocedural MRI versus baseline)—nine out of nine cases; growth (new tissue increase across at least two postprocedural MRIs)—six out of six cases available; stabilization (new tissue unchanged across at least two postprocedural MRIs; that is, a

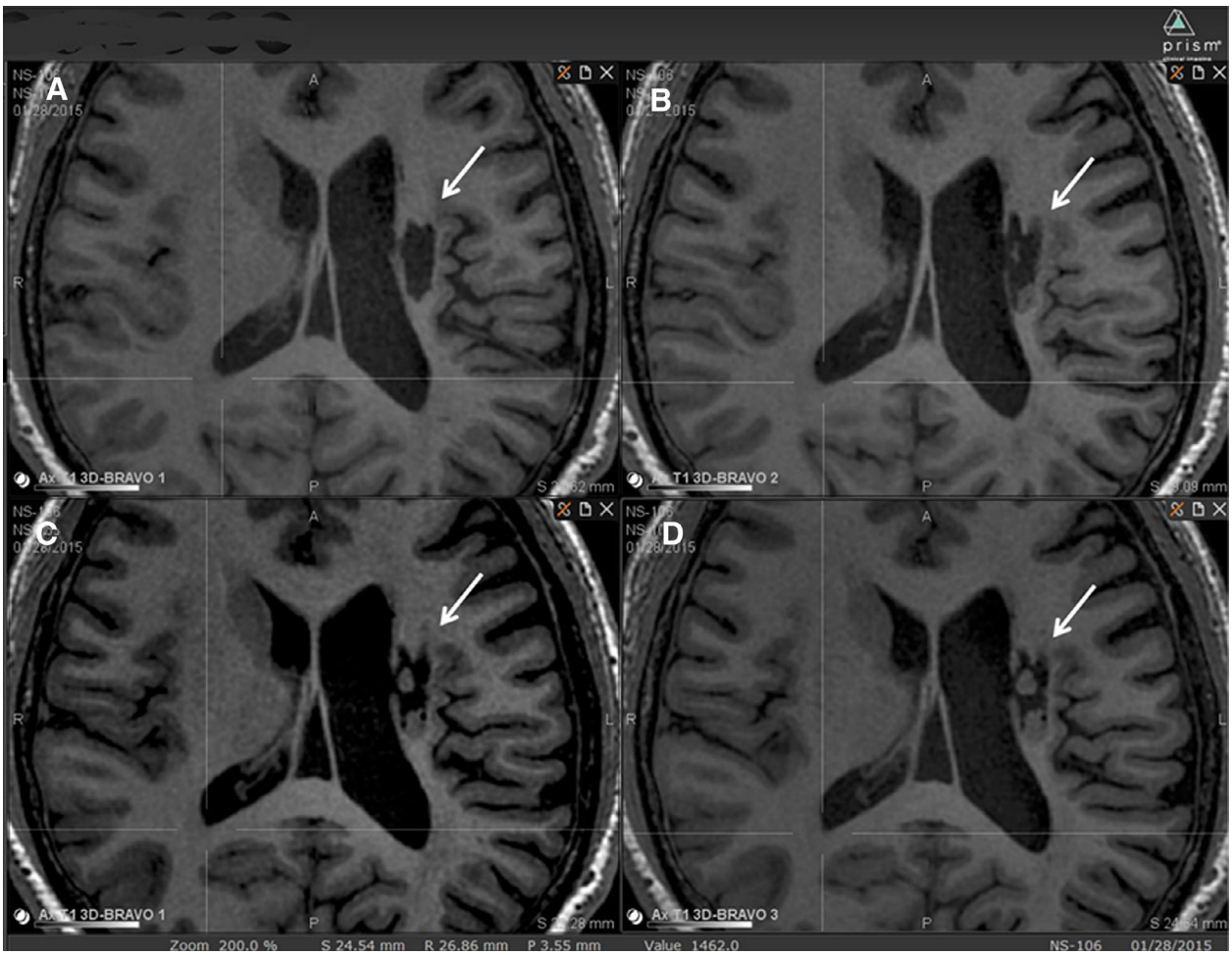

Figure 2. An example of longitudinal MRI of intracavitary tissue growth. A subject from group B (#106) visualized on T1 MRI over time is shown. **(A):** At baseline, **(B)** at 6-month visit, **(C)** at 12-month visit, **(D)** at 24-month visit. The infarct cavity is indicated by an arrow. Two tissue clumps, not present at baseline, presumed to derive from implanted NSI-566, are seen appearing to fill the cavity slowly over time.

growth plateau, up to 24 months)—five out of six cases available; long-term viability beyond 24 months not available. An example of longitudinal MRI of intracavitary tissue growth is shown in Figure 2. Such extraneous tissue presence within infarct cavity was obvious in all nine subjects (Fig. 3).

Quantitative analyses of imaging data were performed as follows: (a) evaluation of lesion (site of implantation) versus surround tissue characteristics through time: the objective was to test the hypothesis that postimplantation tissue changes in the area of implantation reduce the difference between lesion center and unimplanted surround tissue characteristics, (b) evaluation of crossed cerebellar diaschisis (CCD) through time: the objective was to test the hypothesis that tissue changes at the site of implantation may reverse the secondary impact of stroke on brain tissue remote from the site (diaschisis), in this case the cerebellum, and (c) evaluation of tractography at follow-up: the objective was to identify traceable white matter tracts outside of the lesion cavity that changed over time in individual subjects. Imaging measurements were performed in Prism View (Prism Clinical Imaging, Inc., Elm Grove, WI, USA RRID:SCR_016977).

Evaluation of Lesion Versus Surround

To assess the hypothesis that tissue changes were evident after implantation, the lesion versus surround measures at time zero (prior to implantation) were compared with follow-up imaging results for changes in voxel intensity (see Supporting Information for the method). Comparison of lesion-free tissue samples would theoretically produce the ratio of 1. The group mean ratios are shown in Table 4. There were significant changes ($p < .05$) in the difference between the lesion center and its surrounding tissue at one or more follow-up times in T1, fractional anisotropy (FA), mean diffusivity (MD), and cerebral blood flow (CBF) signals with $n = 9$ and positron emission tomography (PET) signal with $n = 8$ (one subject [#105] did not receive a follow-up PET scan). The results suggest significant tissue change in the lesion area versus the surrounding area.

CCD

Seven of the nine subjects exhibited obvious CCD upon visual examination of PET studies at time of implantation, with cerebellar hypometabolism contralateral to the hemisphere containing the stroke lesion. Two subjects (#108, #109) showed negligible differences upon visual examination. Contralateral PET samples were significantly lower than ipsilateral samples both at baseline ($p = .0029$, $n = 9$) and follow-up ($p = .0214$, $n = 8$), confirming that fluorodeoxyglucose (FDG)-(PET does reflect the CCD effect. Perfusion and diffusion parameters, however, were not significantly different. To assess the hypothesis

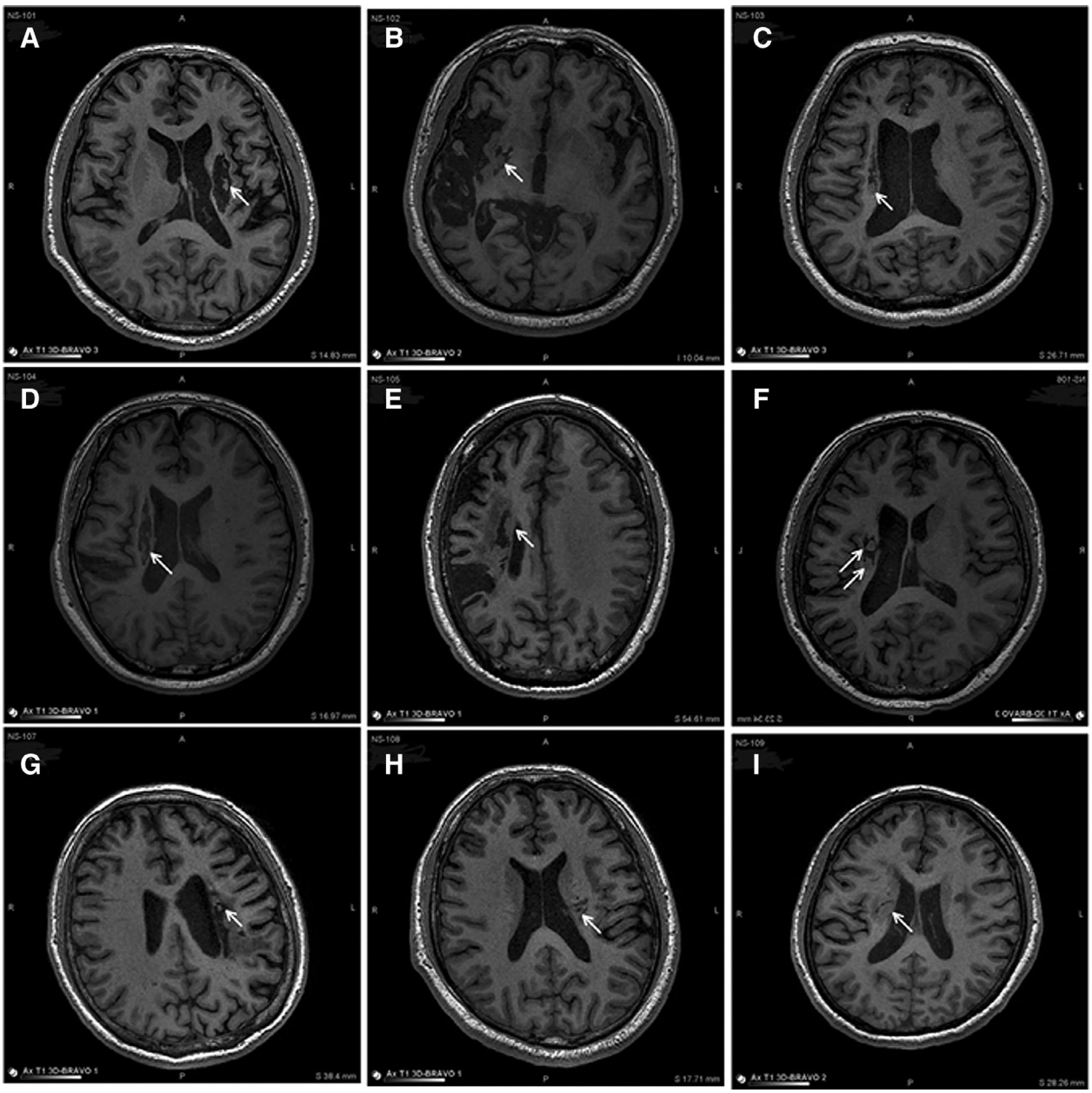

Figure 3. MRI of infarct site at the latest follow-up visit post-NSI-566 transplantation. Shown are all nine subjects (#101–109) visualized on T1 MRI at their latest follow-up post-NSI-566 transplantation. The infarct cavity location is indicated by an arrow. **(A):** #101, at 24 months, **(B)** #102, at 12 months, **(C)** #103, at 14 months, **(D)** #104, at 9 months, **(E)** #105, at 14 months, **(F)** #106, at 24 months, **(G)** #107, at 21 months, **(H)** #108, at 12 months, and **(I)** #109, at 14 months. Growth of new tissue in the infarct cavity is evident in all nine cases.

that cerebellar tissue changes suggestive of a resolution of CCD were evident after implantation, the asymmetry at time zero (implantation) was compared with the asymmetry of the last follow-up imaging results (12 or 24 months). Single-tail paired *t* test revealed no significant change in the difference between the ipsilateral and contralateral (CCD-affected) cerebellum by FA, MD, CBF ($n = 9$), or by PET ($n = 8$; data not shown).

Tractography

Global tractography was created for each baseline and last follow-up (12 or 24 months) diffusion tensor imaging (DTI) ($b = 1{,}000$) scan. Fiber Assignment by Continuous Tracking streamline tracking was performed. In all nine subjects, global tracking (i.e., for the entire brain volume) was visually examined for the presence of major tracts such as the corticospinal tract, which appeared consistent with brain atlas at both baseline and follow-up. Lesion tracking within the cavity was further evaluated by using the lesion voxels as seeds for tractography. Whether the new tracts in the cavity could be traced to identifiable endogenous tracts and how much of the new tracts might appear to be from the graft were assessed. In four subjects, no tracking resulted within the cavity either at baseline or at follow-up. In the remaining five subjects (#101, 104, 106, 108, 109), tracking resulted at the periphery of the lesion in both baseline and follow-up. There was no consistent difference in the number of tracks or tracking course between baseline and follow-up. In

Table 4. Ratio of signal between the stroke lesion center and its surrounding tissue

Visit time (month)	T1 signal				FA signal				MD signal				CBF signal				FDG-PET signal			
	Lesion: surround				Lesion: surround				Lesion: surround				Lesion: surround				Lesion: surround			
	Mean	SD	*n*	*p*[a]	Mean	SD	*n*	*p*[a]	Mean	SD	*n*	*p*[a]	Mean	SD	*n*	*p*[a]	Mean	SD	*n*	*p*[a]
0	0.586	0.140	9		0.438	0.121	9		1.811	0.246	9		0.835	0.105	9		0.737	0.118	9	
6–10	0.729	0.129	9	.007	0.582	0.141	9	.008	1.520	0.316	9	.016	0.894	0.072	7	.130	Nd	Nd	Nd	Nd
10–20	0.712	0.134	9	.016	0.571	0.140	8	.014	1.523	0.181	8	.005	0.911	0.088	7	.039	0.848	0.071	8	.006
>20	0.769	0.151	6	.003	0.600	0.193	6	.021	1.509	0.364	6	.014	0.879	0.086	5	.044	0.844	0.044	4	.042

[a]By *t* test (single tail) between baseline (time 0) and a subsequent visit.
Abbreviation: nd, not done.

some subjects, there were substantially overlapping tracks between baseline and follow-up (#106, 108, 109), which likely represent white matter tracts present prior to intervention and are not from the de novo growth within the lesion seen in other types of images (Supporting Information Fig. S2).

Motor Task Functional MRI

Consistent performance of the motor task was overall lacking. Compliance was also adversely affected by the subjects' apparent difficulty in segregating left versus right motor function, complicating detection of actual cortical reorganization. Thus, functional MRI (fMRI) was not analyzed.

In all subjects, intracavitary tissue showed no evidence of hypermetabolism, relative to cortex. In some cases, intracavitary tissue was too small to assess the degree of metabolism, whereas in others, low metabolic activity similar to white matter was observed. Tissue MD increased in the postinfarct cavities in all subjects but did not match typical healthy white matter or gray matter. Likewise, T1-signal and fluid attenuated inversion recovery (FLAIR)-signal, and T2-signal did not match healthy gray or white matter. There was no evidence of intracavitary or perilesional increase in ASL signal relative to gray matter that might indicate hyperperfusion, neovascularity, and/or hypermetabolism, which was either unobservable or close to white matter in signal intensity. An example of radiological changes is shown in Supporting Information Figure S3.

Discussion

Safety and Maximum Tolerated Dose

NSI-566 is an epigenetically expanded line of primary human neural stem cells (hNSCs) isolated from a single fetal spinal cord tissue. To the best of our knowledge, this is the first study to assess the feasibility and safety of transplanting primary hNSCs into stroke brain in chronic stage. One objective was to determine the maximum tolerated dose (MTD) into the peri-infarct sites in chronic stroke patients. MTD was assumed by three different factors: (a) the maximum cell density that could be prepared for reproducible injection of viable cells, (b) the maximum volume of cell suspension at the maximum cell density to be safely delivered without causing undue compression on the surrounding tissue, and (c) the maximum feasible number of brain penetrations for depositing the cell suspension at strategic locations. Delivery of 72 million cells distributed across 45 deposits via three penetration tracks was safe. Based on the imaging data of new tissue generation in infarct cavity, further dose escalation based on stroke volume may be another variable to test in future studies in optimizing a maximum therapeutic dose for an individual patient.

Two reports of acute cholecystitis by one patient were the only serious AEs recorded for the study. Although rated as unrelated by the investigator, cyclosporine and tacrolimus are known to be associated with an increased incidence of biliary diseases [24].

Extent of Therapeutic Effects

FMMS improvement of 10 points is considered clinically meaningful [25, 26]. From the average of all participants across the doses (n = 9), the change from baseline in FMMS was 16 points at 12 months, which remained stable to 24 months. This result is further corroborated by the improvement measured by the Modified Rankin Scale as well as by the NIHSS. This result is encouraging to move forward to a randomized, sham surgery-controlled, double-blind study with a larger cohort size.

It is unknown how long after the injury the brain can retain plasticity and the capability to reorganize neuromuscular communication. It is commonly assumed that this capability decreases with time after injury. Therefore, in this study, we had arbitrarily limited the chronic injury period to no more than 24 months poststroke. Eight participants had their stroke event 12–24 months prior to the stem cell transplantation, while one was at 5 months prior to transplantation. The observations here indicate that the study population is responsive to the hNSC treatment and appropriate for future hNSC trials. We plan to test the time of hNSC treatment poststroke, age, and gender as covariates in future studies.

Potential Mechanism of Therapeutic Action

Several clinical studies have been reported which evaluated transplantation of other types of cells into basal ganglia of chronic motor stroke patients with similar characteristics to our study [27–31]. One was bone-marrow derived cells genetically modified to transiently overexpress Notch-1 protein [27]. The other was an immortalized line from a fetal neural tissue [28, 32]. The presumed mechanism of therapeutic action by these cells is unclear but thought to involve suppression of inflammation.

Throughout various animal studies, one outstanding property of NSI-566 has been its robust neurogenic potential in vivo, reflected by their ability to send out/receive long-distance projections and integrate with the host tissue [10, 11, 33]. Thus, NSI-566 has shown the ability to provide neurotrophic support via paracrine factors, achieve synaptic integration with host neurons, and promote regeneration of host neuronal fibers [5, 10, 11]. From ALS clinical studies, NSI-566 transplants survive for long periods with only transient immunosuppression in HLA-unmatched recepients [17]. Thus, these neurotrophic/neuroregenerative actions by NSI-566 are expected to be long lasting.

In this study, the facts that, long after cessation of immunosuppressant (first 4 weeks), new tissues appeared and continued to survive in the stroke lesion where NSI-566 had been injected and that the clinical effects persisted throughout 24 months suggest that the mode of action by NSI-566 is regeneration rather than anti-inflammation, although immunomodulatory effects cannot be ruled out and could explain some of the changes seen in imaging. Long-term survival of NSI-566 in ALS patients with only transient immunosuppression has been observed by autopsy [17] as well as by clinical effects [18]. A recent study in SCI primates has also demonstrated a regenerative pathway in which synaptic integration of NSI-566 neurons with host circuitry resulted in motor recovery [11].

New tissue observed on MRI was present within subcortical stroke cavities at the initial 6-month postprocedural MRI for all nine subjects. Cells were injected into white matter surrounding postinfarct cavities, and not directly into the cavities. The new tissues appear to originate from injection sites in the border of cavity. The absence of supranormal metabolic activity on FDG-PET/CT or supranormal signal at ASL perfusion within intracavitry and pericavitary tissues, supports the idea that the new tissue growth is not aggressive. Still, the data cannot prove 100% tissue stability or its origin at this time.

In a phase I study of CTX0E03, a neural tissue-derived immortalized clonal cell line transplanted into a similar subcortical location in chronic stroke patients, researchers described hyperintensity around the needle injection tract on MRI T2-FLAIR images [28]. In our study, T1 as well as T2 FLAIR imaging at follow-up versus baseline did not identify hyperintensity along the needle tracts. The changes were in the infarct and peri-infarct areas.

In animal studies of SCI, traumatic brain injury, and ischemic stroke, implantation of NSI-566 during acute or subacute period has consistently produced cavity-filling tissue by the cells [8–11, 13, 34]. Still, it is surprising that such cavity-filling effect is observed in a human brain tissue lesioned 2 years prior to the cell implantation. This suggests that the human brain may remain malleable for regeneration for 2 years or more.

The macromolecular environment and microstructure of the implanted stem cell tissue is unknown, but differs from either gray matter or white matter. New intracavitary tissue did not exactly follow gray matter or white matter tissue profiles at standard MRI (T1-signal, FLAIR-signal, and T2-signal) or DTI (MD). This may indicate atypical cell structure, atypical myelination, and/or reactive glial response, which are expected of an ectopic hNSC-derived tissue. Quantitative analyses of the lesion (cavity) and surrounding tissue over time in T1, FA, MD, CBF, and FDG-PET parameters indicate significant changes in the lesion toward the surrounding tissue by all parameters at 12 and 24 months. Motor task fMRI was too variable to be analyzed, reflecting the difficulty of acquiring task fMRI in varying degrees of hemiparetic stroke patients. We will explore incorporation of task-free resting-state fMRI in future studies.

PET/CT imaging revealed that intracavitary and pericavitary tissue were hypometabolic relative to gray matter, and closer to white matter when it was observable. Remote pathology due to stroke, CCD, showed significant hypometabolism in cerebellum contralateral to the stroke hemisphere in FDG-PET in some participants. Although intra/pericavity PET signal improved toward the surround nonlesional signal, there were no significant changes in the cerebellar PET signal over time. Thus, anatomical changes appear to be confined within the proximity of the stem cell implantation. Adjuntive physical rehabilitation may improve this situation.

Tractography was also conducted over the 24 months. In five participants, new tracts were identifiable but could not be traced into or out of the cavity. This is not altogether surprising, as tracking is limited in spatial resolution (order of millimeters) and assumes organized, tract-like structure of white matter. The absence of tracking suggests that any new, functional neural connections do not possess the multicellular organization of intact white matter tracts. The trend of white matter-related parameters, such as fractional anisotropy to change in the direction of functioning white matter, still supports the possibility that new neural tissue has formed. One possible mode of action may be that any stem cell-derived tissue is largely composed of interneurons and glia, which promote regeneration of the existing circuitry and serve as bridges between such regenerating neuronal fibers. Such effect of NSI-566 had been observed in a rat model of ischemic SCI [12] as well as in a nonhuman primate model of traumatic SCI [11].

Conclusion

Transplantation of human spinal cord-derived neural stem cells into the peri-infarct area in stable stroke patients was well tolerated and suggested preliminary clinical benefits as measured by three different clinical outcome measures. Results from imaging studies indicate new neural tissue formation in the stem cell implantation area. These results warrant a larger, randomized, controlled, double-blind study.

Acknowledgments

We thank Drs. Douglas Kondziolka and Lawrence R. Wechsler for their help with the initial design of study protocol. We thank the Safety Monitoring Board members: Zhiwen Zhang (Department of Neurosurgery, First Hospital Affiliated to the Chinese PLA General Hospital), Zhenyu Wang (Department of Neurosurgery, Peking University Third Hospital), Pingyan Chen (Department of Biostatistics, School of Public Health and Tropical Medicine, Southern Medical University), Xugui Chen (Department of Anesthesiology, Affiliated BaYi Brain Hospital, Army General Hospital of PLA), Shihong Zhu (Department of ICU, Army General Hospital of PLA), and Hui Jiao (Department of Neurology, Affiliated BaYi Brain Hospital, Army General Hospital of PLA). Statistical analysis was conducted by SynteractHCR and JSS Medical Research India. This work was supported by Neuralstem, Inc.

Author Contributions

GZZ: patient recruitment, surgery, data acquisition, analysis, and interpretation; YL and NL: patient recruitment, neurological evaluations, data acquisition; CYW, JPL, SSX, FW, and TGH: cell manufacturing, delivery, quality assurance, data acquisition; MC, HTZ, YWD, PH, PZ, JHH, HRF, XDL: surgery, data acquisition; JLR and JLU: imaging data analysis and interpretation; KKJ and RXX: conception, design, data analysis and interpretation, supervision of study conduct and operations.

Disclosure of Potential Conflicts of Interest

K.K.J. declared employment, patent holder, research funding, and stock ownership with Neuralstem, Inc. T.G.H. declared

employment, patent holder, and stock ownership with Neuralstem, Inc. J.L.R. declared employment with Prism Clinical Imaging, Inc. J.L.U. declared consultant role for Neuralstem, Inc. J.L., S.X., and F.W. are contractors retained by Suzhou Neuralstem Biopharmaceutics, Ltd., a wholly owned subsidiary of Neuralstem, Inc. The other authors indicated no potential conflicts of interest.

Data Availability Statement

The data that support the findings of this study are available from Neuralstem, Inc. Restrictions apply to the availability of these data, which were used under license for this study. Data are available from kjohe@neuralstem.com with the permission of Neuralstem, Inc.

References

1 Johe KK, Hazel TG, Muller T et al. Single factors direct the differentiation of stem cells from the fetal and adult central nervous system. Genes Dev 1996;10:3129–3140.

2 Shyu, W-C., Lin, S-Z., Wang, H-J., Johe, KK. Methods for treating and/or reversing neurodegenerative diseases and/or disorders. Patent no.: US 9540611B2. 2017.

3 Yan J, Xu L, Welsh AM et al. Combined immunosuppressive agents or CD4 antibodies prolong survival of human neural stem cell grafts and improve disease outcomes in amyotrophic lateral sclerosis transgenic mice. Stem Cells 2006; 24:1976–1985.

4 Xu L, Yan J, Chen D et al. Human neural stem cell grafts ameliorate motor neuron disease in SOD-1 transgenic rats. Transplantation 2006;82:865–875.

5 Xu L, Ryugo DK, Pongstaporn T et al. Human neural stem cell grafts in the spinal cord of SOD1 transgenic rats: Differentiation and structural integration into the segmental motor circuitry. J Comp Neurol 2009;514:297–309.

6 Xu L, Shen P, Hazel T et al. Dual transplantation of human neural stem cells into cervical and lumbar cord ameliorates motor neuron disease in SOD1 transgenic rats. Neurosci Lett 2011;494:222–226.

7 Hefferan M, Galik J, Kakinohana O et al. Human stem cell replacement therapy for amyotrophic lateral sclerosis by spinal transplantation. PLoS One 2012;7:e42614.

8 Yan J, Xu L, Welsh AM et al. Extensive neuronal differentiation of human neural stem cell grafts in adult rat spinal cord. PLoS Med 2007;4:e39.

9 van Gorp S, Leerink M, Kakinohana O et al. Amelioration of motor/sensory dysfunction and spasticity in a rat model of acute lumbar spinal cord injury by human neural stem cell transplantation. Stem Cell Res Ther 2013; 4:57.

10 Lu P, Wang Y, Graham L et al. Long-distance growth and connectivity of neural stem cells after severe spinal cord injury. Cell 2012;150:1264–1273.

11 Rosenzweig ES, Brock JH, Lu P et al. Restorative effects of human neural stem cell grafts on the primate spinal cord. Nat Med 2018;24:484–490.

12 Cizkova D, Kakinohana O, Kucharova K et al. Functional recovery in rats with ischemic paraplegia after spinal grafting of human spinal stem cells. Neuroscience 2007;147:546–560.

13 Tajiri N, Quach DM, Kaneko Y et al. Behavioral and histopathological assessment of adult ischemic rat brains after intracerebral transplantation of NSI-566RSC cell lines. PLoS One 2014;9:e91408.

14 Glass JD, Hertzberg VS, Boulis NM et al. Transplantation of spinal cord-derived neural stem cells for ALS: Analysis of phase 1 and 2 trials. Neurology 2016;87:392–400. [Erratum in: Neurology 2017;89:521].

15 Feldman EL, Boulis NM, Hur J et al. Intraspinal neural stem cell transplantation in amyotrophic lateral sclerosis: Phase 1 trial outcomes. Ann Neurol 2014;75:363–373.

16 Glass JD, Boulis NM, Johe K et al. Lumbar intraspinal injection of neural stem cells in patients with amyotrophic lateral sclerosis: Results of a phase I trial in 12 patients. Stem Cells 2012;30:1144–1151.

17 Tadesse T, Gearing M, Senitzer D et al. Analysis of graft survival in a trial of stem cell transplant in ALS. Ann Clin Transl Neurol 2014;1:900–908.

18 Goutman S, Brown M, Glass J et al. Long-term phase 1/2 intraspinal stem cell transplantation outcomes in ALS. Ann Clin Transl Neurol 2018;5:730–740.

19 Curtis E, Martin R, Gabel B et al. A first-in-human, phase I study of neural stem cell transplantation for chronic spinal cord injury. Cell Stem Cell 2018;22:941.e6–950.e6.

20 Wang W, Jiang B, Sun H et al. Prevalence, incidence, and mortality of stroke in china: Results from a nationwide population-based survey of 480,687 adults. Circulation 2017;135:759–771.

21 Kondziolka D, Steinberg GK, Cullen SB et al. Evaluation of surgical techniques for neuronal cell transplantation used in patients with stroke. Cell Transplant 2004;13:749–754.

22 Bjarkam CR, Glud AN, Margolin L et al. Safety and function of a new clinical intracerebral microinjection instrument for stem cells and therapeutics examined in the Göttingen minipig. Stereotact Funct Neurosurg 2010;88:56–63.

23 Glud AN, Bjarkam CR, Azimi N et al. Feasibility of three-dimensional placement of human therapeutic stem cells using the intracerebral microinjection instrument. Neuromodulation 2016;19:708–716. [Erratum in: Neuromodulation 2016;19:904].

24 Stief J, Stempfle HU, Götzberger M et al. Biliary diseases in heart transplanted patients: A comparison between cyclosporine A versus tacrolimus-based immunosuppression. Eur J Med Res 2009;14:206–209.

25 Gladstone DJ, Danells CJ, Black SE. The Fugl-Meyer assessment of motor recovery after stroke: A critical review of its measurement properties. Neurorehabil Neural Repair 2002; 16:232–240.

26 Page SJ, Fulk GD, Boyne P. Clinically important differences for the upper-extremity Fugl-Meyer Scale in people with minimal to moderate impairment due to chronic stroke. Phys Ther 2012;92:791–798.

27 Steinberg GK, Kondziolka D, Wechsler LR et al. Clinical outcomes of transplanted modified bone marrow-derived mesenchymal stem cells in stroke: A phase 1/2a study. Stroke 2016; 47:1817–1824.

28 Kalladka D, Sinden J, Pollock K et al. Human neural stem cells in patients with chronic ischaemic stroke (PISCES): A phase 1, first-in-man study. Lancet 2016;388:787–796.

29 Chen DC, Lin SZ, Fan JR et al. Intracerebral implantation of autologous peripheral blood stem cells in stroke patients: A randomized phase II study. Cell Transplant 2014; 23:1599–1612.

30 Shin YK, Cho SR. Exploring erythropoietin and G-CSF combination therapy in chronic stroke patients. Int J Mol Sci 2016; 17:463.

31 Kondziolka D, Steinberg GK, Wechsler L et al. Neurotransplantation for patients with subcortical motor stroke: A phase 2 randomized trial. J Neurosurg 2005;103:38–45.

32 Stroemer P, Patel S, Hope A et al. The neural stem cell line CTX0E03 promotes behavioral recovery and endogenous neurogenesis after experimental stroke in a dose-dependent fashion. Neurorehabil Neural Repair 2009;23: 895–909.

33 Usvald D, Vodicka P, Hlucilova J et al. Analysis of dosing regimen and reproducibility of intraspinal grafting of human spinal stem cells in immunosuppressed minipigs. Cell Transplant 2010;19:1103–1122.

34 Spurlock MS, Ahmed AI, Rivera KN et al. Amelioration of penetrating ballistic-like brain injury induced cognitive deficits after neuronal differentiation of transplanted human neural stem cells. J Neurotrauma 2017;34:1981–1995.

See www.StemCellsTM.com for supporting information available online.